Published in final edited form as:
Magn Reson Med. 2009 May ; 61(5): 1015–1021. doi:10.1002/mrm.21854.

Simultaneous measurement of pulmonary partial pressure of oxygen and apparent diffusion coefficient by hyperpolarized ^{3}He MRI

Jiangsheng Yu[1], **Michelle Law**[1], **Stephen Kadlecek**[1], **Kiarash Emami**[1], **Masaru Ishii**[2], **Michael Stephen**[1], **John M. Woodburn**[1], **Vahid Vahdat**[1], and **Rahim R. Rizi, PhD**[1]

[1] Department of Radiology, University of Pennsylvania, Philadelphia, PA, USA

[2] Department of Otolaryngology-Head and Neck Surgery, Johns Hopkins University, Baltimore, MD, USA

Abstract

Hyperpolarized ^{3}He (HP ^{3}He) MRI shows promise to assess structural and functional pulmonary parameters in a sensitive, regional and non-invasive way. Structural HP ^{3}He MRI has applied the *apparent diffusion coefficient* (ADC) for the detection of disease-induced lung microstructure changes at the alveolar level, and HP ^{3}He *pulmonary partial pressure of oxygen* (pO_2) imaging measures the oxygen transfer efficiency between the lung and blood stream. Although both parameters are affected in chronic obstructive pulmonary disease (COPD), a quantitative assessment of the regional correlation of the two parameters has not been reported in the literature. In this work, a single acquisition technique for the simultaneous measurement of ADC and pO_2 is presented. This technique is based on the multiple regression method, in which a general linear estimator is used to retrieve the values of ADC and pO_2 from a series of measurements. The measurement uncertainties are also analytically derived and used to find an optimal measurement scheme. The technique was first tested on a phantom model, and then on an *in-vivo* normal pig experiment. A case study was performed on a COPD patient, which showed that in a region-of-interest ADC was 29% higher while oxygen depletion rate was 61% lower than the corresponding global average values.

Keywords

Hyperpolarized ^{3}He MRI; apparent diffusion coefficient; partial pressure of oxygen; multiple regression method

Introduction

Chronic obstructive pulmonary disease (COPD), a group of diseases that includes chronic bronchitis and emphysema, accounts for substantial health care spending and is the fourth leading cause of death in the United States(1). Conventional methods to diagnose and evaluate COPD include pulmonary function tests (PFTs) and computed tomography (CT). PFTs only provide a gross assessment of the state of the disease, and their application is largely limited to qualitative, clinical diagnosis. X-ray computed tomography (CT) can detect and stage the diseases with only limited sensitivity and is not suitable for long-term

Address of corresponding author: Rahim R. Rizi, PhD, Department of Radiology, University of Pennsylvania, MMRRCC, B1 Stellar-Chance Bldg, 422 Curie Blvd, Philadelphia, PA, USA, 19104, rizi@uphs.upenn.edu, Tel./Fax.: 215-573-3866 / 215-573-2113.

studies due to radiation exposure(2–5). In general, magnetic resonance imaging (MRI) provides superior soft tissue contrast when compared to other imaging modalities. However, conventional proton-based MRI of the lung suffers from poor signal-to-noise ratios due to low proton density and susceptibility gradients between airways and tissue. In recent years, hyperpolarized ^{3}He (HP ^{3}He) MRI techniques have been studied extensively and have become promising tools to assess structural and functional pulmonary parameters in a sensitive, regional and non-invasive way(6–8).

Structural HP ^{3}He MRI has relied heavily on a measurement called the *apparent diffusion coefficient* (ADC), which is a function of alveolar size and geometry, to characterize the lung's microstructure at the alveolar level(9–13). This technique utilizes the fact that the atoms of ^{3}He gas have a restricted diffusion capability in the lung because the alveolar size (~200μm) is smaller than the free diffusion mean distance during a time period encoded into the imaging pulse sequence. Therefore, the measured diffusion coefficient in the lung is substantially smaller than the free diffusion coefficient and depends sensitively on the local alveolar and small airway dimensions. The alveolar size in emphysema patients increases as a consequence of lung tissue destruction caused by the disease. Tissue destruction allows ^{3}He atoms greater freedom to move, so it is expected that these patients will have a large measured ADC value. A number of studies have demonstrated significant difference between the ^{3}He ADC values measured in healthy and emphysematous subjects (9,11,12,14). The most common technique used for ADC measurement is to introduce a bipolar gradient to sensitize the received signal intensity to the diffusion effect. This gradient pulse is implemented after the longitudinal magnetization is flipped to the transverse plane and before the MRI signal is acquired (15). The logarithm of the diffusion-induced signal attenuation is proportional to both the ADC value and the so-called gradient factor, a function of gradient timing and magnitude that represents the bipolar gradient strength.

The HP ^{3}He MRI pulmonary oxygen measurement, an example of functional imaging, which seeks to image physiological parameters other than the anatomic and pathological description of lung structure, yields alveolar partial pressure of oxygen (pO_2) and oxygen depletion rate (R) (16–19). In the presence of oxygen, the hyperpolarized magnetization of ^{3}He gas will gradually decay due to the dipolar couplings between the ^{3}He's nuclear spins and the electronic spins of paramagnetic oxygen molecules(20). When ^{3}He gas is inhaled into the lung, the decay rate is proportional to the pulmonary partial pressure of oxygen if other slower depolarization processes (e.g. ^{3}He-^{3}He dipolar coupling and interactions with the tissue) are ignored(16). This T_1 dependence of hyperpolarized ^{3}He on local oxygen concentration provides the basis for measuring the pulmonary partial pressure of oxygen and oxygen depletion rate. These two parameters are sensitive markers of oxygen transfer efficiency between the lung airspaces and the pulmonary blood(3). Therefore, an accurate, regional mapping of pO_2 and R with HP ^{3}He MRI can enhance the detection of the pulmonary function changes associated with COPD.

There is considerable interest in investigating the correlation between lung structure and function parameters in patients with COPD. Various researchers have applied the CT technique to study the link between lung structure and regional pulmonary ventilation. These studies show that in addition to causing structural changes, COPD also directly affects lung ventilation through irreversible airflow limitation. To date, the investigation of the correlation between lung structure changes and oxygen exchange efficiency has not been reported in the literature.

In this study, we present a single-acquisition technique for the simultaneous measurement of pO_2, R and ADC. This technique provides a co-registered measurement between the

pulmonary structure and oxygen exchange efficiency, and may give new insight into the pathophysiologic mechanisms of COPD. We believe that physicians may be able to use the co-registered measurement to accurately diagnose early disease-induced changes in lung function and structure, quantitatively follow disease progression, and immediately ascertain response to therapy. Performing a simultaneous measurement also saves expensive ^{3}He gas and shortens measurement time. The latter is especially beneficial to the patient, as it reduces the breath-hold time.

This simultaneous measurement technique is based on the multiple regression method, in which the general least square estimator is used to retrieve pO_2, R and ADC values from a series of acquired signals. The measurement uncertainty of each parameter is also analytically derived. An optimal measurement scheme which yields minimal uncertainties in pO_2, R and ADC is found through numerical simulation. The simultaneous measurement technique was first tested on a phantom model, and then on a normal animal model. Finally, a case study was performed on a patient with severe COPD to investigate the correlation between pO_2, R and ADC.

Theory

In the simultaneous measurement of the pulmonary partial pressure of oxygen and ADC using HP ^{3}He MRI, three factors contribute to the signal evolution of a series of acquired images. First, the presence of oxygen in the lung will impose a decay on the hyperpolarized longitudinal magnetization. Second, the bipolar gradient used for sensitizing the diffusion effect will cause a transverse magnetization attenuation. The third factor is the radio-frequency (RF) pulse, which flips the hyperpolarized longitudinal magnetization to the transverse plane for spatial encoding and signal acquisition. The signal evolution of a series of images acquired by a small flip angle gradient echo sequence can be expressed as:

$$S_n = S_0 \cdot (\cos\alpha)^{Nn} \cdot \exp\left[-\frac{1}{\xi}\int_0^{t(n)} p_{O_2}(t)dt\right] \cdot \exp(-b(n)\cdot D), \quad [1]$$

where S_0 and S_n are the signal intensities of the initial and the n^{th} image; $(\cos\alpha)^{Nn}$ represents the RF effect, where α is the flip angle and N is the number of phase coding steps of an image; $\exp\left[-\frac{1}{\xi}\int_0^{t(n)} p_{O_2}(t)dt\right]$ represents the decay due to oxygen, where $p_{O_2}(t)$ is the time-dependent partial pressure of oxygen in the lung, $t(n)$ is the time at which the acquisition of n^{th} image is completed, and ζ =1976.0 Torr·s is the oxygen-induced longitudinal relaxation coefficient at body temperature; and $\exp(-b(n)\cdot D)$ represents the diffusion effect, where D is the apparent diffusion coefficient, and $b(n)$ is the bipolar gradient factor introduced in the n^{th} image.

During a breath-hold, the time evolution of partial pressure of oxygen in the lung can be accurately approximated as a linear function of time(16):

$$p_{O_2}(t) = p_0 - R\cdot t, \quad [2]$$

where p_0 is the initial oxygen partial pressure and R is the oxygen depletion rate, the speed at which oxygen is dissolved from the alveoli into the blood. Substituting Eq.[2] into Eq.[1] and normalizing S_n with respect to the initial signal S_0, Eq.[1] can be expressed as:

$$E_n=\ln(S_n/S_0)=\varepsilon\cdot n-\frac{1}{\xi}\cdot p_0\cdot t(n)+\frac{1}{2\xi}\cdot R\cdot t^2(n)-D\cdot b(n), \quad [3]$$

where$\varepsilon = N\cdot\ln(\cos\alpha)$.

In Eq.[3], the normalized signal E_n is a linear summation of the four unknown parameters ε, p_0, R and D, multiplied by the respective associated coefficients n, $t(n)$, $t^2(n)$ and $b(n)$. Based on Appendix 1, the multiple regression method can be applied to recover the values of the four parameters from a series of measurements(21–23), which gives:

$$[\varepsilon, p_0, R, D]^T=(X^T\cdot V\cdot X)^{-1}\cdot X^T\cdot V\cdot y, \quad [4]$$

where X is the coefficient matrix, V is the signal matrix, and y is normalized signal vector:

$$X=\begin{bmatrix}1 & t_1 & t_1^2 & b_1\\ 2 & t_2 & t_2^2 & b_2\\ \vdots & \vdots & \vdots & \vdots\\ n & t_n & t_n^2 & b_n\end{bmatrix};\ V=\begin{bmatrix}S_1^2 & 0 & \cdots & 0\\ 0 & S_2^2 & 0 & \vdots\\ \vdots & 0 & \ddots & 0\\ 0 & \cdots & 0 & S_n^2\end{bmatrix};\ y=\begin{bmatrix}y_1\\ y_2\\ \vdots\\ y_n\end{bmatrix}.$$

In the four column vectors of the coefficient matrix X, the first vector will be linearly dependent on the second vector if the measurement timing $t(n)$ is a linear function of n. In this case, the inverse of X does not exist and Eq.[4] yields no solution. Similarly, the fourth vector, which represents the gradient factor $b(n)$, also needs to be linearly independent of the first vector. This means when the single-acquisition technique is applied to measure p_0, R and ADC simultaneously, the measurement timing cannot be evenly-spaced and the gradient factors cannot be evenly increasing or decreasing. Intuitively, the three effects of oxygen, ADC and RF can be separated only when each effect contributes to the total signal evolution in different patterns by which the coefficients progress.

In Eq.[4], to recover p_0, R and ADC from a single-acquisition measurement, the choice of measurement timing $t(n)$ and gradient factors $b(n)$ are not restricted except that neither can linearly vary with n. However, in the presence of measurement noise, different choices of $t(n)$ and $b(n)$ will yield significant differences on the measurement uncertainties of p_0, R and ADC. The uncertainties of p_0, R and ADC can be derived according to the error propagation theorem and expressed as(23):

$$\left[\sigma_\varepsilon^2,\sigma_{p_0}^2,\sigma_R^2,\sigma_D^2\right]^T=\sigma^2\cdot(X^T\cdot V\cdot X)^{-1}. \quad [5]$$

From Eq.[5], finding optimal $t(n)$ and $b(n)$ to minimize measurement uncertainties $\sigma_{p_0}^2,\sigma_R^2,\sigma_D^2$ is a multi-variable and multi-target optimization problem. The signal matrix V is dependent on scan parameters such as flip angle and phase encoding steps, as seen in Eq.[1]. This dependence complicates the problem and makes an analytical solution difficult to obtain. In our study, a numerical simulation was used to evaluate the noise performances of a variety of measurement schemes in order to choose an optimal scheme that yields minimal measurement uncertainties in p_0, R and ADC. To simplify the problem, the gradient factors $b(n)$ were first set to progress according to:

$$b(n)=b_0(\sqrt{M}-\sqrt{n}), \quad [6]$$

where b_0 is the base gradient factor and M is the number of images in the series.

Since $b(n)$ in Eq.[6] decreases with n, small gradient factors are applied in the last several images, in which signal-to-noise ratios are low because the hyperpolarized longitudinal magnetization is already substantially consumed by the oxygen and RF effects. In addition, the square-root function used in Eq.[6] allows the gradient factor to vary in a smaller range than it would in other possible choices (e.g. polynomial functions), thereby guaranteeing that the maximum gradient amplitude of the scanner will not be exceeded. After determining the gradient factors $b(n)$, the numerical simulation can apply a similar procedure as described in Ref.(24), in which the measurement timing and flip angle are optimized to minimize the measurement uncertainties of p_0 and R. From a variety of choices, the numerical simulation found the timing scheme that optimized the measurements of p_0 and R also yielded a minimal measurement uncertainty on ADC. As shown in Fig. 1, the inter-scan time of this optimal timing scheme is relatively long in the middle and short at the two ends of the measurement. The simulation showed that the normalized measurement uncertainty (standard deviation over mean value) was 14.2% for p_0, 84.2% for R and 15% for ADC when this optimal timing scheme was used under the following measurement condition: an initial ^{3}He polarization yielding a SNR=120 for the first image at α =2.5 degrees, b_0 =1.4 s/cm^2, N=64, number of images=6, breath-hold duration=20s, p_0 =106 Torr, R =1.9 Torr/s and ADC=0.2 cm^2/s. The optimal flip angle of this scheme is 3.6 degrees for p_0, 4.4 degrees for R and 4.0 degrees for ADC (In practice, only one flip angle is used for each measurement because the optimal flip angles for the three parameters are close enough).

Materials and methods

Polarized ^{3}He production and administration

A commercial-prototype polarizer (Amersham Health, Durham, NC) was used to generate hyperpolarized ^{3}He gas. The polarization process is based on the optical pumping mechanism, in which the angular momentum of circularly polarized light is first transferred to the electronic spins of Rubidium (Rb) atoms and then to the nuclear spins of ^{3}He atoms(25–27). A batch volume of one liter of ^{3}He gas with a polarization level of approximately 30% can be achieved after 10 hours of optical pumping. In the experiments, ^{3}He gas was dispensed from the polarizer, stored in a plastic bag, transferred to the scanner, and administered immediately before the imaging sequence was initiated.

Phantom experiment

The simultaneous measurement technique was first tested on a phantom model which simulated a free diffusion environment. An 18×18 cm^2 plastic bag was filled with a mixture of gas consisting of (500±20)ml HP ^{3}He and (110±3)ml O_2. The bag was loosely contained in a fixed holder and the gas pressure in the bag was balanced with the atmospheric pressure of the environment. The nominal partial pressure of oxygen was approximately 110/(500+110) (bar) * 760 (Torr/bar) ≈ 137 Torr. The bag was also tightly sealed to simulate an oxygen depletion rate of zero.

A commercial birdcage RF coil (Rapid Biomedical, Würzburg, Germany) was used in the experiment. The coil was 35 cm long and 27 cm in diameter, and operated in quadrature mode. The experiment was conducted at a Siemens Sonata 1.5T MRI system and the coil was tuned to the ^{3}He resonance frequency 48.48 MHz. The MRI pulse sequence used for

imaging was a small flip angle gradient echo sequence with a diffusion-sensitization bipolar gradient introduced in the readout direction. A series of six images was acquired with the timing scheme [0, 0.64, 10.68, 20.72, 25.76, 28.80] (seconds) and the gradient factor set [0, 0.49, 0.33, 0.20, 0.09, 0] (s/cm^2). To prevent the signal from becoming over-attenuated by the high free diffusion coefficient, the gradient factor set in the phantom experiment was much smaller than the set in the animal experiment. In the phantom experiment, a field of view (FOV) of 300mm and a single slice of 100mm thickness were used in order to cover the whole volume of the bag and avoid a polarization diffusion refresh from the neighboring region on the RF-excited slice. The other scan parameters were: TR/TE:10ms/6.26ms, matrix size: 64×64, image resolution: 4.69mm × 4.69mm, and flip angle=2.4 degrees.

Animal experiment

The animal experiment was conducted under a protocol approved by the Institutional Animal Care and Use Committee at the University of Pennsylvania. A 22 kg Yorkshire pig was sedated with ketamine and placed supine inside the 1.5T Siemens Sonata MRI scanner. The RF coil was the same as the one used in the phantom experiment. The animal was ventilated with a home-built prototype ventilator. A tidal volume of 500ml gas mixture, consisting of 100ml O_2 and 400ml ^3He gas, was administered to the pig immediately before the simultaneous measurement was initiated. A series of six images were acquired for a single slice with the timing scheme [0, 1.92, 13.24, 24.56, 30.88, 35.20] (seconds) and the gradient factor set [0, 1.73, 1.15, 0.71, 0.33, 0] (s/cm^2). The imaging parameters used in the diffusion-sensitization gradient echo sequence were: FOV=240mm; slice thickness=30mm; TR/TE:10ms/6.26ms, matrix size: 64×64, image resolution: 3.75mm × 3.75mm, and flip angle=3.0 degrees. After the simultaneous measurement, separated measurements on partial pressure of oxygen and ADC were performed. The gas mixture used was 100ml O_2, 300ml ^3He and 100ml N_2 for the separated partial pressure of oxygen measurement, and 200ml ^3He and 300ml N_2 for the separated ADC measurement. In the separated partial pressure of oxygen measurement, a gradient echo sequence was used without the bipolar diffusion-sensitization gradient.

Human experiment

The human experiment was conducted under an IRB-approved protocol and a US FDA IND. A patient with severe COPD (female, age 52 years, weight ~50kg) was imaged on a 1.5T Siemens Sonata MRI system. The subject's total lung capacity (TLC) was 6.08 liters. In the experiment, the subject inhaled a 900ml (15%×TLC) gas mixture consisting of 500ml ^3He, 180ml O_2 and 220ml nitrogen (N_2). The RF coil used for imaging was a transmitter-receiver ^3He saddle coil set (IGC Medical Advances Inc., Milwaukee, WI, USA), which was composed of two coils (each 23cm×25cm) and operated in quadrature mode. For the simultaneous p_0, R and ADC measurement, a series of six images were acquired for a single slice with the timing scheme [0, 1.32, 9.04, 16.06, 21.08, 24.10] (seconds) and the gradient factor set [0, 1.73, 1.15, 0.71, 0.33, 0] (s/cm^2). The imaging parameters used in the diffusion-sensitization gradient echo sequence were: FOV=350mm; slice thickness=50mm; TR/TE:10ms/6.96ms, matrix size: 64×64, and flip angle=4.6 degrees.

Data analysis

The multiple regression method which applied the general least square estimator for p_0, R and ADC calculation was implemented in Matlab (Mathworks Inc. USA). In the data analysis, the signals of the acquired images were first bias-corrected from the background noise(28,29):

$$S_n = \sqrt{\bar{S}_n^2 - \sigma^2}, \quad [7]$$

where $\bar{S}_n$ and S_n denote the signal intensities before and after the correction, respectively, and σ is the original MRI noise in S_n. σ can be calculated from $\sigma = \sqrt{\frac{2}{\pi}}\bar{M}$, where $\bar{M}$ is the mean value of a 5×5 region at the right-bottom corner of the image where no signal is contained. To generate the parametric maps of p_0, R and ADC, the image pixels were grouped into 2×2 bins, and a bin-by-bin fitting was performed according to Eq.[4]. Two thresholds were applied to select the valid bins. The average threshold only chose bins with an average SNR greater than 3.0 for analysis. The homogeneity threshold selected bins in which the ratio of standard deviation of pixel intensities over the average was smaller than 0.4, and therefore excluded the bins at the edge of the lung where only parts of the bin contained signals.

Results

Phantom experiment

As shown in Fig. 2, the measured average p_0 value was 145±7 Torr, which agreed with the nominal value 137 Torr. The small discrepancy was likely caused by the small volume variance in the administered gas mixture (the gas mixture consisting of (500±20)ml HP ^{3}He and (110±3)ml O_2). The average of the measured R values was 0.03±0.43 Torr/s, close to the expected value 0.0 Torr/s. The phantom experiment was meant to simulate a free diffusion environment, but due to the presence of 20% O_2 in the gas mixture, the measured average ADC value was (1.51±0.08)cm^2/s, which is in good agreement with the value (1.60 ± 0.05) cm^2/s measured at the same gas concentration by Kober *et. al.* (30).

Animal experiment

The fitted parametric maps of the normal pig experiment are shown in Fig. 3, which shows that the average values of p_0, R and ADC are 79±15 Torr, 2.1±0.7 Torr/s and 0.14±0.06 cm^2/s, respectively. The separate pulmonary oxygen and ADC measurements that followed the simultaneous measurement yielded an average value of 80±12 Torr for p_0, 2.0±0.5 Torr/s for R, and 0.14±0.05 cm^2/s for ADC, which were consistent with the values of the simultaneous measurement.

Human experiment

The experiment results for the COPD patient are shown in Fig. 4, in which the average values of p_0, R and ADC are listed on the corresponding parametric maps. In the figure, the left lung showed low signal intensity due to the poor ventilation caused by the disease. In the selected region-of-interest (the white square box) in the right lung, the measured average ADC was 0.85cm^2/s, which was significantly higher than the reported ADC value (0.20cm^2/s) of normal subjects(9,10), and the measured R value was 1.2 Torr/s, smaller than the normal oxygen depletion rate of 2.5 Torr/s(16,18). It is also worth noting that in the region-of-interest, ADC was (0.85-0.66)/0.66=29% higher than the global ADC average value while R was (3.1-1.2)/3.1=61% lower than the global R average value. This correlation suggests that oxygen exchange efficiency was affected in the region where lung tissue was destroyed by COPD.

Discussion

As seen in Eq.[3], four unknown parameters, ε, p_0, R and D, need to be recovered from a series of measurements in the simultaneous measurement technique. Consequently, at the same measurement conditions, the simultaneous measurement technique will introduce higher measurement uncertainties on the p_0, R and ADC than the separated partial pressure of oxygen and ADC measurements(21). At the experiment condition described at the end of the theory section, the simulation showed that for the simultaneous measurement, the normalized measurement uncertainty (standard deviation over mean value) was 14.2% for p_0, 84.2% for R and 15% for ADC. These values are higher than the uncertainties obtained during separate partial pressure of oxygen and ADC measurements: 7.5% for p_0, 56.1% for R and 9.6% for ADC.

A straightforward way to reduce measurement uncertainties is to increase the signal-to-noise ratios of the acquired images. In fact, Eq.[5] indicates that the measurement uncertainties of p_0, R and ADC are inversely proportional to the signal-to-noise ratios (SNRs). If there is no room left to improve the initial ^{3}He hyperpolarization, two techniques may be used to increase the SNRs of the acquired images. The first one, called the pre-wash technique, uses multiple inhales and exhales to increase the ^{3}He gas concentration inside the lung before the simultaneous measurement is initiated. This technique, which was originally applied to measure the regional fractional ventilation of the lung, causes the signal to build up approximately linearly for the first few breaths, saturating after ~5–10 pre-washes(31). If images are also taken at each step of the pre-wash, a scheme that simultaneously measures fractional ventilation, p_0, R and ADC can be implemented. The second technique to improve SNRs is to imprint the diffusion effect onto the longitudinal magnetization using the stimulated echo technique. By avoiding the insertion of the conventional bipolar gradient for diffusion sensitization, a short TE can be chosen in the MRI pulse sequence to increase the SNRs (T2* in the lung is ~8ms). The stimulated echo technique was used by Mugler et. al. to measure the long range diffusion coefficient(32). Therefore, when applying this technique, it is possible to measure p_0, R and long range diffusion coefficient simultaneously.

Conclusion

In this work, we present a single-acquisition technique for the simultaneous measurement of p_0, R and ADC. This technique is based on the multiple regression method, which applies the general linear estimator to retrieve the values of p_0, R and ADC from a series of acquired images. The measurement uncertainties are also analytically derived. Numerical simulation was performed to find an optimal measurement scheme from a variety of choices. This technique was first tested on a phantom model, and then in an *in-vivo* normal pig experiment. A case study was performed on a COPD patient to investigate the correlation between p_0, R and ADC, which showed that in a region-of-interest ADC is 29% higher while R is 61% lower than the corresponding global average values.

Acknowledgments

Grants: NIH grants R01-HL064741, R01-HL077241, R21-EB005241.

References

1. Barnes PJ. Chronic Obstructive Pulmonary Disease. N Engl J Med 2000;343(4):269–280. [PubMed: 10911010]
2. Gurney J. Pathophysiology of obstructive airways disease. Radiol Clin North Am 1998;36:15–27. [PubMed: 9465866]

3. West, J. Respiratory physiology:the essentials. Baltimore, MD: Lippincott Williams & Wilkins; 1999.
4. Newell JDHJ Jr, Snider GL. Report of a workshop: quantitative computed tomography scanning in longitudinal studies of emphysema. Eur Respir J 2004;23:769–775. [PubMed: 15176695]
5. Thurlbeck WMMN. Emphysema: definition, imaging, quantification. Am J Roentgenol Radium Ther 1994;163:1017–1025.
6. Bachert P, Schad LR, Bock M, Knopp MV, Ebert M, Grossman T, Heil W, Hofmann D, Surkau R, Otten EW. Nuclear magnetic resonance imaging of airways in humans with use of hyperpolarized ^{3}He. Magnetic Resonance in Medicine 1996;36(2):192–196. [PubMed: 8843371]
7. MacFall JR, Charles HC, Black RD, Middleton H, Swartz JC, Saam B, Driehuys B, Erickson C, Happer W, Cates GD, Johnson GA, Ravin CE. Human lung air spaces: potential for MR imaging with hyperpolarized ^{3}He. Radiology 1996;200(2):553–558. [PubMed: 8685356]
8. de Lange EE, Mugler JPI, Brookeman JR, Knight-Scott J, Truwit JD, Teates CD, Daniel TM, Bogorad PL, Cates GD. Lung air spaces: MR imaging evaluation with hyperpolarized ^{3}He gas. Radiology 1999;210(3):851–857. [PubMed: 10207491]
9. Saam BT, Yablonskiy DA, Kodibagkar VD, Leawoods JC, Gierada DS, Cooper JD, Lefrak SS, Conradi MS. MR imaging of diffusion of ^{3}He gas in healthy and diseased lungs. Magn Reson Med 2000;44:174–179. [PubMed: 10918314]
10. Yablonskiy DA, Saam BT, Gierada DS, Lefrak SS, Cooper JD, Conradi MS. Quantitative in vivo assessment of lung microstructure at the alveolar level with hyperpolarized ^{3}He diffusion MRI. Proc Natl Acad Sci U S A 2002;99:3111–3116. [PubMed: 11867733]
11. Salerno M, de Lange EE, Altes TA, Truwit JD, Brookeman JR, Mugler JPI. Emphysema: hyperpolarized ^{3}He diffusion MR imaging of the lungs compared with spirometric indexes- initial experience. Radiology 2002;222(1):252–260. [PubMed: 11756734]
12. Mayo JR, Hayden ME. Hyperpolarized ^{3}He diffusion imaging of the lung. Radiology 2002;222:8–11. [PubMed: 11756698]
13. Jiangsheng Yu MI, Kadlecek Stephen, Lipson David A, Emami Kiarash, Brainard Benjamin M, Clark Timothy W, Rajaei Sheeva, Rizi Rahim R. Multiple Regression Method for Pulmonary Apparent Diffusion Coefficient Measurement by Hyperpolarized 3He MRI. 2007;25:982–991.
14. Salerno M, Altes TA, Brookeman JR, de Lange EE, Mugler JPI. Rapid hyperpolarized ^{3}He diffusion MRI of healthy and emphysematous human lungs using an optimized interleaved-spiral pulse sequence. J Magn Reson Imaging 2003;17(5):581–588. [PubMed: 12720268]
15. Stejskal EO. Use of Spin Echoes in a Pulsed Magnetic-Field Gradient to Study Anisotropic, Restricted Diffusion and Flow. J Chem Phys 1965;43(10):3597–3603.
16. Deninger AJ, Eberle B, Ebert M, Grossmann T, Heil W, Kauczor HU, Lauer L, Markstaller K, Otten E, Schmiedeskamp J, Schreiber W, Surkau R, Thelen M, Weiler N. Quantification of regional intrapulmonary oxygen partial pressure evolution during apnea by ^{3}He MRI. J MagnReson 1999;141(2):207–216.
17. Fischer MC, Spector ZZ, Ishii M, Yu J, Emami K, Itkin M, Rizi RR. Single-acquisition sequence for the measurement of oxygen partial pressure by hyperpolarized gas MRI. Magn Reson Med 2004;52(4):766–773. [PubMed: 15389934]
18. Wild JM, Fichele S, Woodhouse N, Paley MNJ, Kasuboski L, van Beek EJR. 3D Volume-Localized pO_2 Measurement in the Human Lung with ^{3}He MRI. Magn Res Med 2005;53(5): 1055–1064.
19. Eberle B, Weiler N, Markstaller K, Kauczor HU, Deninger AJ, Ebert M, Grossmann T, Heil W, Lauer LO, Roberts TPL, Schreiber WG, Surkau R, Dick WF, Otten EW, Thelen M. Analysis of intrapulmonary O_2 concentration by MR imaging of inhaled hyperpolarized ^{3}He. Journal of Applied Physiology 1999;87(6):2043–2052. [PubMed: 10601148]
20. Saam B, Happer W, Middleton H. Nuclear relaxation of ^{3}He in the presence of O_2. Phys Rev A 1995;52(1):862–865. [PubMed: 9912313]
21. Bevington P. RDK. Data Reduction and Error Analysis for the Physical Sciences 2003;40–41:102–104.
22. Berger GCaRL. Statistical Inference. Duxbury Press; 2001.
23. Hayashi, F. Econometrics. Princeton University Press; 2000. p. 54-58.

24. Yu, Jiangsheng; Ishii, Masaru; Law, Michelle; Woodburn, John M.; Emami, Kiarash; Kadlecek, Stephen; Vahdat, Vahid; Guyer, Richard A.; Rizi, RR. Optimization of scan parameters in pulmonary partial pressure oxygen measurement by hyperpolarized 3He MRI Magnetic Resonance in Medicine. 2008;59(1):124–131.
25. Ben-Amar Baranga A, Appelt S, Romalis MV, Erickson CJ, Young AR, Cates GD, Happer W. Polarization of ^{3}He by Spin Exchange with Optically Pumped Rb and K Vapors. Phys Rev Lett 1998;80:2801–2804.
26. Bouchiat MA, Carver TR, Varnum CM. Nuclear polarization in ^{3}He gas induced by optical pumping and dipolar exchange. Physical Review Letters 1960;5:373–375.
27. Walker TG, Happer W. Spin-Exchange Optical Pumping of Noble-Gas Nuclei. Rev Mod Phys 1997;69(2):629–642.
28. Henkelman RM. Measurement of signal intensities in the presence of noise in MR images. Med Phys 1985;12(2):232–233. [PubMed: 4000083]
29. Gudbjartsson H, Patz S. The Rician distribution of noisy MRI data. Magn Reson Med 1995;34:910–914. [PubMed: 8598820]
30. Kober FBK, Belle V, Viallon M, Leviel JL, Delon A, Ziegler A, Décorps M. NMR Imaging of Thermally Polarized Helium-3 Gas. Journal of Magnetic Resonance 1999;138:308–312. [PubMed: 10341135]
31. Deninger AJ, Mansson S, Petersson JS, Pettersson G, Magnusson P, Svensson J, Fridlund B, Hansson G, Erjefeldt I, Wollmer P, Golman K. Quantitative measurement of regional lung ventilation using ^{3}He MRI. Magn Reson Med 2002;48(2):223–232. [PubMed: 12210930]
32. Chengbo Wang GWM, Altes Talissa A, de Lange Eduard E, Cates Gordon D Jr, Mugler John P III. Time Dependence of 3He Diffusion in the Human Lung: Measurement in the Long-Time Regime Using Stimulated Echoes. Magnetic Resonance in Medicine 2006;56:296–309. [PubMed: 16791861]

Appendix 1

General least square fitting minimizes the following weighted square summation(21–23):

$$\chi^2=\sum_{n=1}^{M}\frac{1}{\sigma_n^2}(y_n-E_n)^2=\sum_{n=1}^{M}\frac{1}{\sigma_n^2}\left[y_n-\left(\varepsilon\cdot n-\frac{1}{\xi}p_0\cdot t(n)+\frac{1}{2\xi}R\cdot t^2(n)-D\cdot b(n)\right)\right]^2 \tag{A.1}$$

where M is the number of images acquired after the initial image in the series, y_n denotes the normalized measured signal intensity, and σ_n is the noise in y_n. The weighted summation reflects that after normalization the noise σ_n is not uniform. Based on the error propagation theorem, the noise σ_n in y_n is related to the original MRI noiseσ in S_n by:

$$\sigma_n^2=\frac{1}{S_n^2}\sigma^2+\frac{1}{S_0^2}\sigma^2\approx\frac{1}{S_n^2}\sigma^2 \tag{A.2}$$

This approximation is valid because, from Eq.[1], $S_0 \gg S_n$.

Eq.(A.1) can be expressed in matrix form:

$$\chi^2=(Cy-CX\beta)^T(Cy-CX\beta) \tag{A.3}$$

where C is the noise matrix, y is the vector of normalized signals, X is the coefficient matrix, and β is the vector of unknown parameters:

$$C=\begin{bmatrix} 1/\sigma_1 & 0 & \cdots & 0 \\ 0 & 1/\sigma_2 & 0 & \vdots \\ \vdots & 0 & \ddots & 0 \\ 0 & \cdots & 0 & 1/\sigma_n \end{bmatrix};y=\begin{bmatrix} y_1 \\ y_2 \\ \vdots \\ y_n \end{bmatrix};X=\begin{bmatrix} 1 & t_1 & t_1^2 & b_1 \\ 2 & t_2 & t_2^2 & b_2 \\ \vdots & \vdots & \vdots & \vdots \\ n & t_n & t_n^2 & b_n \end{bmatrix};\beta=\begin{bmatrix} \varepsilon \\ p_0 \\ R \\ D \end{bmatrix}.$$

The minimum value of χ^2 can be reached by setting to zero the partial derivatives of Eq.(A. 3) with respect to β:

$$\frac{\partial \chi^2}{\partial \beta}=-(CX)^T(Cy-CX\beta)+(Cy-CX\beta)^T(-CX)=-2X^TX^TCy+2X^TC^TCX\beta=0$$

Therefore,

$$\beta=(X^TC^TCX)^{-1}X^TC^TCy=(X^T\cdot V\cdot X)^{-1}\cdot X^T\cdot V\cdot y$$

Here we define the signal matrix $V=C^TC=\begin{bmatrix} S_1^2 & 0 & \cdots & 0 \\ 0 & S_2^2 & 0 & \vdots \\ \vdots & 0 & \ddots & 0 \\ 0 & \cdots & 0 & S_n^2 \end{bmatrix}$ by utilizing Eq.[A.2].

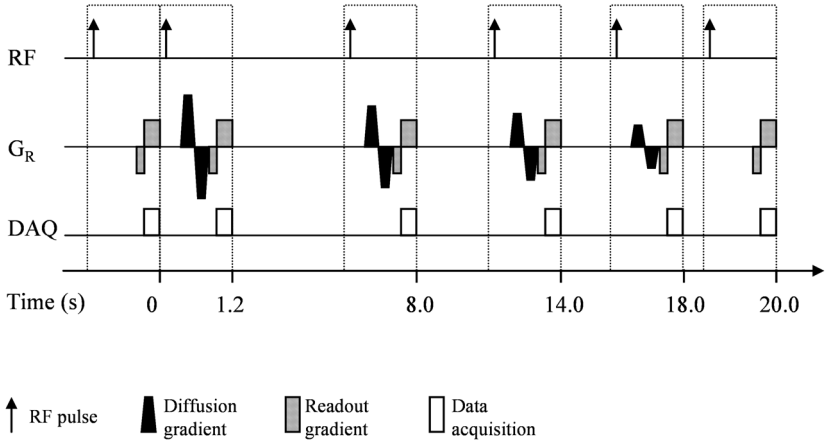

Fig. 1.

Schematic diagram of the optimal measurement scheme for the simultaneous measurement of p_0, R and ADC with HP ^{3}He MRI. The inter-scan time of this scheme is relatively long in the middle and short at the two ends. The bipolar diffusion-sensitization gradient is applied along the readout direction. Its magnitude decreases with the measurement. For simplicity, the slice selection and phase coding gradient are not shown in the figure.

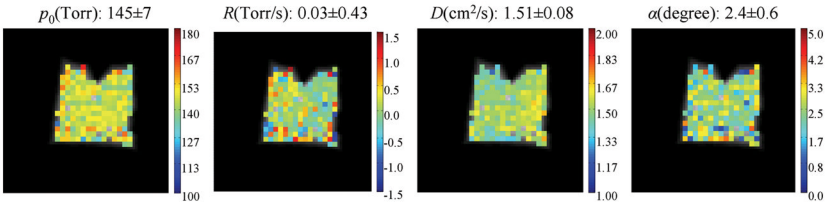

Fig. 2.

Simultaneous measurement of p_0, R and ADC with HP ^{3}He MRI on a phantom model. The phantom was an 18×18 cm^2 plastic bag filled with a gas mixture consisting of 500ml HP ^{3}He and 110ml O_2, to simulate a free ^{3}He diffusion environment. The expected nominal values are 137Torr for p_0 and 0.0Torr/s for R.

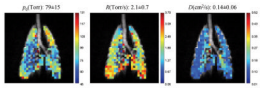

Fig. 3.

Simultaneous measurement of p_0, R and ADC with HP ^{3}He MRI on an *in-vivo* normal pig experiment. The tracheal region was excluded from data fitting due to a low signal-to-noise ratio caused by high diffusion coefficient. The separated measurements that followed the simultaneous measurement yielded an average value of 80±12 Torr for p_0, 2.0±0.5 Torr/s for R, and 0.14±0.05 cm^2/s for ADC.

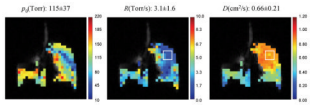

Fig. 4.

A case study of simultaneous measurement of p_0, R and ADC with HP ^{3}He MRI on a COPD patient. In the selected region-of-interest (white square box), the ADC is 29% higher while R is 61% lower than the corresponding global average values. A correlation between the two parameters suggests that in the region where lung tissue was destroyed by COPD, the oxygen exchange efficiency was also reduced.